

Substrate-Specific Heterogeneous Catalysis of CeO₂ by Entropic Effects via Multiple Interactions

Masazumi Tamura,^{*,†} Kyoichi Sawabe,[¶] Keiichi Tomishige,[†] Atsushi Satsuma,^{¶,§} and Ken-ichi Shimizu^{*,‡,§}

[†]Department of Applied Chemistry, Graduate School of Engineering, Tohoku University 6-6-07, Aoba, Aramaki, Aoba-ku, Sendai 980-8579, Japan

[¶]Department of Molecular Design and Engineering, Graduate School of Engineering, Nagoya University, Nagoya 464-8603, Japan

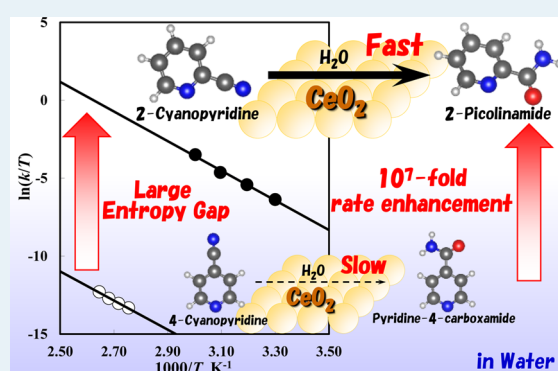
[§]Elements Strategy Initiative for Catalysts and Batteries, Kyoto University, Katsura, Kyoto 615-8520, Japan

[‡]Catalysis Research Center, Hokkaido University, N-21, W-10, Sapporo 001-0021, Japan

S Supporting Information

ABSTRACT: Achieving complete substrate specificity through multiple interactions like an enzyme is one of the ultimate goals in catalytic studies. Herein, we demonstrate that multiple interactions between the CeO₂ surface and substrates are the origin of substrate-specific hydration of nitriles in water by CeO₂, which is exclusively applicable to the nitriles with a heteroatom (N or O) adjacent to the α -carbon of the CN group but is not applicable to the other nitriles. Kinetic studies reveal that CeO₂ reduces the entropic barrier ($T\Delta S^\ddagger$) for the reaction of the former reactive substrate, leading to 10⁷-fold rate enhancement compared with the latter substrate. Density functional theory (DFT) calculations confirmed multiple interaction of the reactive substrate with CeO₂, as well as preferable approximation and alignment of the nitrile group of the substrate to the active OH group on CeO₂ surface. This can lead to the reduction of the entropic barrier. This is the first example of an entropy-driven substrate-specific catalysis of a nonporous metal oxide surface, which will provide a new design strategy for enzyme-inspired synthetic catalysts.

KEYWORDS: cerium oxide, heterogeneous catalysis, hydration, substrate specificity, nitrile



1. INTRODUCTION

Mimicking the catalytic machinery of biological systems in synthetic chemistry is a special challenge for chemists.¹ Enzymes are capable of 10⁶–10¹⁹-fold rate enhancement for reactions of a specific substrate (substrate specificity). The rate enhancement is achieved by multiple interactions (H-bonding, electrostatic interactions, π -stacking, hydrophobic or hydrophilic interactions, etc.) between reactive sites and substrates, which causes transition-state-like conformation of substrates relative to the catalytic centers. In order to achieve substrate-specific organic synthesis, various enzyme-inspired artificial catalysts have been reported.² Despite great efforts being made in this field, achieving the sufficient level of selectivity comparable to enzymes is still challenging even in molecular catalysis. Bols and co-workers^{2d,e} exemplified the highest substrate specificity (193-fold rate enhancement) for hydrolysis of nitrophenyl glycosides using cyclodextrin derivatives. However, the level is far from that of enzymes. The substrate specificity in similar sized substrates is more challenging. Baba and co-workers,^{2g} and Maruoka and co-workers^{2f} demonstrated efficient cage-shaped homogeneous catalysts, which showed the high substrate specificity (28-fold and 11-fold, respectively). On the other hand, unmodified

inorganic catalysts such as metal oxides usually have difficulty in achieving enzyme-like substrate specificity. Porous materials such as zeolites,³ microporous heteropolyacids,⁴ TiO₂-incorporated porous SiO₂,⁵ and microporous titanosilicate⁶ can recognize large differences in the substrate sizes mainly by repulsive steric effects using the rigid pocket. However, the substrate specificity (<10³-fold) is far from that of enzymes, and these systems cannot recognize a slight difference in the substrate structure. Organic-functionalized porous materials⁷ were also reported, which however suffer from the same problems as above. In order to recognize the slight difference between the substrates with a similar structure like structural isomers, Tada and co-workers⁸ and Katz and co-workers⁹ successfully developed well-designed molecular-imprinted SiO₂ modified with organic function groups and/or metal complexes, where both repulsive steric effect between the substrate and SiO₂-wall and attractive interaction between the substrate and the catalytic species worked effectively to afford the substrate specificity

Received: September 23, 2014

Revised: November 5, 2014

Published: November 7, 2014

(10^2-fold). These artificial catalytic systems failed to attain enzyme-level (10^6–10^{19}-fold) rate difference.

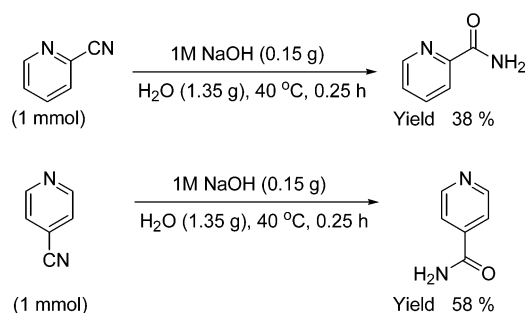
Considerable efforts have been devoted to reveal the mechanism which describes how the enzyme-catalyzed reactions show a higher rate than noncatalyzed systems. For intramolecular reaction, most of the researchers claimed that the main factor of rate enhancement is reduction of the activation enthalpy (ΔH^\ddagger), which is related to stabilization of the transition state.¹⁰ However, for two substrate reactions, an enzyme must gather two substrates from dilute solution and bind them in a configuration that is conducive to reaction. This approximation effect brings about reduction of entropic barrier ($T\Delta S^\ddagger$), which will in principle produce a large rate enhancement.¹¹ Wolfenden and co-workers¹² reported that 10^7-fold rate enhancement in peptide bond formation by ribosome was entirely driven by rendering $T\Delta S^\ddagger$ more preferably without change of ΔH^\ddagger, which indicates that the approximation effect through multiple interactions is responsible for the reduction of the activation barrier (ΔG^\ddagger). The effect of the entropic barrier on the rate difference between different substrates remains unexplored in the fields of both enzyme and artificial catalysis, although studies on the enthalpy/entropy effects on substrate-specific catalysis will afford new concept in molecular recognition in catalysis.

Recently, we reported preliminary results on substrate-specific nitrile hydration in water by a nonporous metal oxide, CeO_2.¹³ 2-Cyanopyridine, as a specific substrate, was quantitatively converted to the corresponding amide under enzymatic conditions (i.e., in water, pH 7, ambient temperature), and the reaction followed pseudo-Michaelis–Menten type kinetics.¹³ In our continuous effort to investigate the mechanism of this system, we report herein that CeO_2 shows significant rate enhancement for hydration of specific nitriles with a heteroatom (N or O) adjacent to the α -carbon of the CN group. The reaction rate of 2-cyanopyridine is 10^7-orders of magnitude higher than that of 4-cyanopyridine, which is achieved entirely by rendering $T\Delta S^\ddagger$, whereas ΔH^\ddagger is similar between these nitriles. DFT study shows that multiple interactions between the reactive substrate and CeO_2 surface, and the approximation and alignment effect are responsible for the unprecedented substrate specificity.

2. RESULTS AND DISCUSSION

Substrate-Specific Catalysis of CeO_2. First, we compared the intrinsic reactivity of 2-cyanopyridine and 4-cyanopyridine for hydration by a conventional base catalyst (1 M NaOH) at 40 °C. Under the conditions in Scheme 1, the reactions of 2-cyanopyridine and 4-cyanopyridine provided the corresponding amides in 38% and 58% yields, respectively. This indicates that the intrinsic reactivity of 4-cyanopyridine for nitrile hydration is

Scheme 1. Hydration of 2-Cyanopyridine and 4-Cyanopyridine by NaOH Catalyst



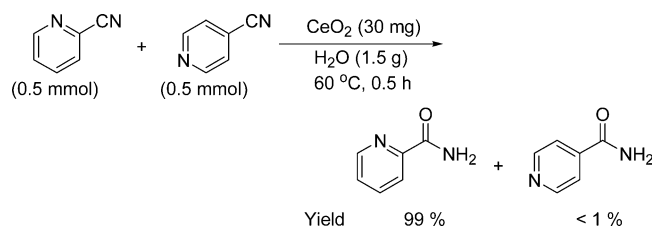
higher than that of 2-cyanopyridine. By contrast, in the presence of CeO_2 (Table 1) 2-cyanopyridine gave higher yield of >99% at 30 °C (entry 1) than 4-cyanopyridine (4%) at 100 °C (entry 11). Next, a competitive reaction using both 2-cyanopyridine and 4-cyanopyridine as substrates was carried out at 60 °C (Scheme 2).

Table 1. Hydration of Various Nitriles over CeO_2^a

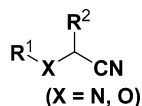
Entry	Nitrile	Amide	T (°C)	t (h)	Yield (%)
1			30	12	>99 (>99 ^b)
2			80	6	>99
3			80	6	97
4			80	6	95
5			30	1	98
6			30	3	92
7 ^b			60	12	94
8			80	24	90
9 ^c			80	24	77
10			100	24	5
11			100	24	4
12			100	24	0
13			100	24	0
14			100	24	0
15			100	24	9
16			100	24	0
17			100	24	0
18			100	24	10
19			100	24	4
20			100	24	23

^aReaction conditions: nitrile (2 mmol), CeO_2 (30 mg), H_2O (3.0 g), air. Yield of amide was determined by GC. ^bSolvent: $\text{H}_2\text{O}/\text{EtOH}$ = 1/1. ^cCeO_2 calcined at 600 °C was used.

Scheme 2. Competitive Hydration of Cyanopyridines



2-Cyanopyridine was converted to the corresponding amide in 99% yield, while 4-cyanopyridine remained intact. To further investigate generality in the substrate-specific catalysis of CeO₂, the scope of substrates for CeO₂-catalyzed nitrile hydration was examined as summarized in Table 1. 2-Cyanopyridine derivatives with various substituents (entries 1–4), cyanopyrazine (entry 5), 2-pyrimidinecarbonitrile (entry 6) and 1-isoquinolinecarbonitrile (entry 7) were effectively hydrated to the corresponding amides in high yields (92 - >99%). Similar reactivity tendency was observed in other catalyst systems,¹⁴ although the difference of the reactivities between reactive substrates and less reactive ones is much smaller than that of CeO₂ system. 2-Furancarboxitrile (entry 8) and methoxyacetonitrile (entry 9) also reacted to afford the corresponding amides in good yields. The reactive substrates (entries 1–9) have a common structure: a heteroatom (N or O) adjacent to the α -carbon of the CN group.



On the other hand, nitriles with a heteroatom adjacent to the β - or γ -carbon of the CN group, 3-cyanopyridine (entry 10), 4-cyanopyridine (entry 11), 2-pyridineacetonitrile (entry 12), 3-furancarboxitrile (entry 13), 3-methoxypropionitrile (entry 14), and 2-quinolinecarbonitrile (entry 15), showed no or less reactivity even at 100 °C. Nitriles without any heteroatoms, valeronitrile (entry 16) and benzonitrile (entry 17), were completely unreactive at 100 °C. These results suggested that a heteroatom (N or O atom) adjacent to the α -carbon of the CN group is indispensable for the progress of the reaction. Furthermore, a slight difference of the structure strongly changes the reactivity. Exceptions for the above classification are shown in entries 18–20, where nitriles with a N atom adjacent to the α -carbon of CN group, dimethylaminoacetonitrile (entry 18), 1-cyanomethylpiperidine (entry 19) and 2-cyanopyrrole (entry 20) gave low reactivity. Comparison of the structures of above reactive nitriles (entries 1–9) with those of dimethylaminoacetonitrile and 1-cyanomethylpiperidine (entries 18 and 19) suggests that the steric hindrance around the N atom adjacent to the α -carbon of the CN group is unfavorable for the reaction. In the case of 2-cyanopyrrole, weaker basicity of N atom of the pyrrole than N atom of pyridine or O atom of furan, which is due to delocalization of the lone pair of N atom in pyrrole through π -conjugation, will be unfavorable for adsorption of the substrate. In summary, tentative conclusions on the structure–reactivity relationship can be drawn as follows:

- (1) Reactive substrates possess a heteroatom (N or O) adjacent to the α -carbon of the CN group, whereas other nitriles are unreactive.
- (2) Exceptions to the above classification are nitriles with sterically hindered substituents at the heteroatom (N or

O) adjacent to the α -carbon of the CN group, which has low reactivity.

Further discussions on these phenomena will be given on the basis of the following studies on kinetics and DFT calculations.

Eyring Plot. To quantitatively discuss the substrate-specific hydration of nitriles by CeO₂, kinetic studies were examined using 2-cyanopyridine and 4-cyanopyridine as model substrates. We previously showed that the reaction of 2-cyanopyridine on CeO₂ follows the Michaelis–Menten type kinetics.¹³ The reaction can proceed via a nitrile–CeO₂ adsorption complex derived from the equilibrium reaction between a free nitrile and CeO₂ surface.

Arrhenius parameters for CeO₂-catalyzed reactions of 2-cyanopyridine and 4-cyanopyridine were compared in Figure S1. Both reactions provided linear Arrhenius plots, and the activation energies (E_a) and the frequency factors (A) for 2-cyanopyridine and 4-cyanopyridine were $81.7 \pm 1.7 \text{ kJ mol}^{-1}$ and $\ln A = 31.7 \pm 0.6$, and $80.7 \pm 13.2 \text{ kJ mol}^{-1}$ and $\ln A = 19.3 \pm 4.3$, respectively. The similar activation energies indicate that the mechanism in hydration of these nitriles is the same in principle. The reaction rate of 2-cyanopyridine at 30 °C was 10⁷-fold higher than that of 4-cyanopyridine, which was calculated by extrapolation of the Arrhenius plot for 4-cyanopyridine. The significant difference in the reactivity originates from large difference in the frequency factors ($\ln A$).

To further discuss the origin of the 10⁷-fold difference in the reactivity, Eyring parameters for the reactions were estimated (Figure 1). The slopes of the Eyring plots for 2-cyanopyridine and 4-cyanopyridine are close to each other, which indicates similar activation enthalpies for these nitriles. Therefore, the

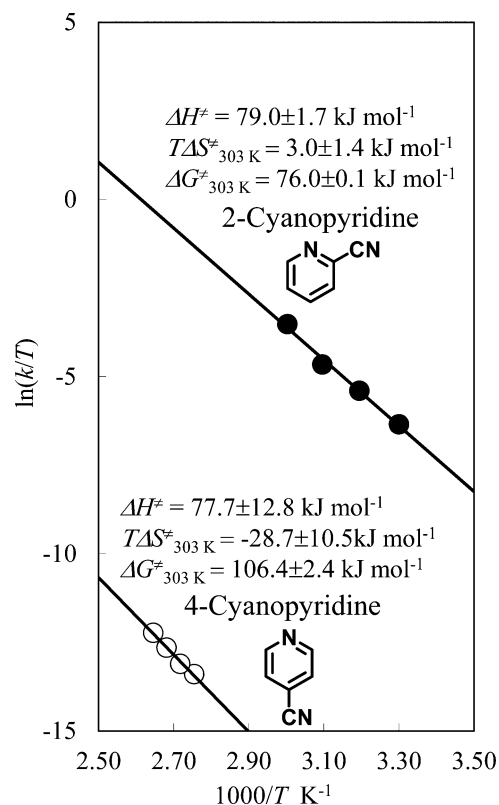
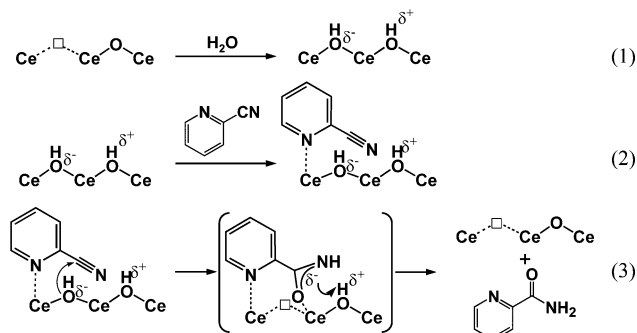


Figure 1. Eyring plots for the hydration of 2-cyanopyridine and 4-cyanopyridine. Reaction conditions: nitrile (1.0 mmol), CeO₂ (30 mg), H₂O (3.0 g).

large difference in the reactivity of these nitriles is mainly derived from the large entropy gap. ΔH^\ddagger , $T\Delta S^\ddagger_{303\text{ K}}$ and $\Delta G^\ddagger_{303\text{ K}}$ (the activation Gibbs energy) for 2-cyanopyridine and 4-cyanopyridine are calculated from the lines as follows: ΔH^\ddagger , $T\Delta S^\ddagger_{303\text{ K}}$ and $\Delta G^\ddagger_{303\text{ K}}$ for 2-cyanopyridine are $79.0 \pm 1.7\text{ kJ mol}^{-1}$, $3.0 \pm 1.4\text{ J mol}^{-1}$ and $76.0 \pm 0.1\text{ kJ mol}^{-1}$, respectively, and those for 4-cyanopyridine are $77.7 \pm 12.8\text{ kJ mol}^{-1}$, $-28.7 \pm 10.5\text{ kJ mol}^{-1}$, and $106.4 \pm 2.4\text{ kJ mol}^{-1}$, respectively. A large difference in activation entropy is responsible for the large difference of $\Delta G^\ddagger_{303\text{ K}}$ between 2-cyanopyridine and 4-cyanopyridine, resulting in the large difference of the reactivity. To the best of our knowledge, the present CeO_2 -catalyzed system is the first report of the artificial catalyst that achieves the enzyme-like (10^7 -fold) substrate specificity, that is driven by a reduction of entropic barrier. In general, ΔS^\ddagger in bimolecular reactions is negative ($-100 \sim -200\text{ J K}^{-1}\text{ mol}^{-1}$). $T\Delta S^\ddagger_{303\text{ K}}$ of 4-cyanopyridine is negative (-28.7 kJ mol^{-1}). On the other hand, $T\Delta S^\ddagger_{303\text{ K}}$ of 2-cyanopyridine is positive (3.0 kJ mol^{-1}), indicating that the conformation of the 2-cyanopyridine adsorbed on CeO_2 is favorable for the reaction. This result suggests that flexibility of 2-cyanopyridine on CeO_2 is decreased by multiple interactions in the initial adsorption state, which is released in the transition state (TS). The positive $T\Delta S^\ddagger_{303\text{ K}}$ for 2-cyanopyridine on CeO_2 is characteristic to the reaction, which will be derived from the gathering of two substrates (H_2O and nitriles) at neighboring active sites on CeO_2 surface in the appropriate configuration. This characteristic over CeO_2 will be responsible for the high reactivity of 2-cyanopyridine.

DFT Calculation of Adsorption States of Substrates. In our previous works¹³ we have proposed the mechanism of CeO_2 -catalyzed hydration of nitriles shown in Scheme 3, which

Scheme 3. Proposed Reaction Mechanism for Hydration of 2-Cyanopyridine on CeO_2



consists of (1) dissociation of H_2O on the exposed $\text{Ce}-\text{O}$ site to give $\text{OH}^\delta-$ and $\text{H}^\delta+$ species on Ce and O sites, (2) formation of nitrile- CeO_2 adduct, (3) addition of $\text{OH}^\delta-$ to the carbon atom of the CN group, and desorption of the amide from the CeO_2 surface, accompanying a regeneration of the $\text{Ce}-\text{O}$ site. Addition of $\text{OH}^\delta-$ to the carbon atom of the CN group is the rate-limiting step. The Eyring parameters in this study indicate that 10^7 -fold higher activity of 2-cyanopyridine than 4-cyanopyridine is due to the lower entropic barriers for 2-cyanopyridine. As mentioned above, the lower entropic barrier will be brought about by the two main factors:^{15,10d} (1) stabilization of the substrates through multiple interactions, (2) approximation and alignment. Approximation and alignment (orientation) are known in the concept of near attack conformation,¹⁶ and shorter distance between the reacting atoms and lower approaching angle to bonding angle are preferable for decrease of ΔG^\ddagger , which leads to

enhancement of the reaction rate. In order to verify the above hypotheses, the adsorption states of the substrates on CeO_2 were examined by DFT calculations.

First, the adsorption state of 2-cyanopyridine was compared with that of 4-cyanopyridine on (111) surface of CeO_2 . The (111) facet of CeO_2 is the most stable one from the thermodynamic viewpoint.¹⁷ Because 2-cyanopyridine and 4-cyanopyridine have two nitrogen atoms which can act as Lewis bases, two adsorption modes on CeO_2 can be assumed: one is adsorption through the N atom of pyridine ring ($\text{N}_{\text{pyridine}}$), and the other one is adsorption through the N atom of nitrile group ($\text{N}_{\text{nitrile}}$). The exposed Ce atom acts as a Lewis acid site on CeO_2 .¹⁸ Furthermore, CeO_2 surface with OH adspecies has several Lewis acid sites due to the difference of environment around Ce atom. Thus, the suitable adsorption site was estimated by adsorption of HCN as the simplest nitrile model on CeO_2 using three sites: (1) Ce atom next to OH adspecies, (2) Ce atom between OH adspecies, and (3) Ce atom apart from OH adspecies (Figure S2). As a result, (1) the Ce atom next to OH adspecies is a suitable adsorption site for the N atom of the substrates, and the N atom on this site interacts with both of Ce and H of OH adspecies. The optimized structures of 2-cyanopyridine and 4-cyanopyridine and their relative energies (ΔE) are shown in Figure 2a–d.¹⁹ Relative energy (ΔE) is defined as the electronic energy of the adsorption system relative to that of the isolated system. Thus, a negative value means an exothermic process. Taking ΔE into consideration, these substrates prefer the adsorption through $\text{N}_{\text{pyridine}}$. This can be explained by the higher basicity of $\text{N}_{\text{pyridine}}$ than $\text{N}_{\text{nitrile}}$. Furthermore, electron density of the adsorption state of 2-cyanopyridine shows triple interactions²⁰ (Figure 3a,b): $\text{N}_{\text{pyridine}}(2\text{-cyanopyridine}) \cdots \text{H}(\text{OH adspecies on CeO}_2)$, $\text{N}_{\text{nitrile}}(2\text{-cyanopyridine}) \cdots \text{H}(\text{OH adspecies on CeO}_2)$ and $\text{H}(\text{pyridine ring of 2-cyanopyridine}) \cdots \text{O}(\text{CeO}_2)$, and the ΔE is -0.49 eV , which is the lowest among the optimized structures. Note that this adsorption site of $\text{N}_{\text{pyridine}}$ is clearly different from that of the proposed reaction mechanism (Scheme 3 and Figure 3b). On the other hand, 4-cyanopyridine is adsorbed only at $\text{N}_{\text{pyridine}}$ and the ΔE is -0.32 eV . These results indicate that larger stabilization of 2-cyanopyridine was caused by the multiple interactions. The reacting atoms (C atom of CN group and O atom of OH adspecies on CeO_2) in the case of 2-cyanopyridine are much closer (3.80 \AA) than that in the case of 4-cyanopyridine (7.02 \AA) (Figure 2a,c) and are also located at favorable positions for the reaction (Figure 3c). For the 2-cyanopyridine- CeO_2 adduct, the $\text{C}\equiv\text{N}$ bond length (1.16 \AA) is the same as that of the isolated 2-cyanopyridine, which indicates that the weak interaction between $\text{N}_{\text{nitrile}}$ and Ce does not change the local electronic structure of the CN group. Thus, the higher reactivity of 2-cyanopyridine than 4-cyanopyridine shown in Figure 1 will be driven by the multiple interactions between 2-cyanopyridine and CeO_2 , as well as the approximation and alignment of the nitrile carbon to oxygen of OH adspecies on CeO_2 .

Similar results were obtained in the case of 1-isoquinoline-carbonitrile (another reactive nitrile, Table 1 entry 7) on CeO_2 (Figure 4).²¹ These results support the above claim that nitriles with a heteroatom adjacent to the α -carbon of the CN group are effective for the reaction through multiple interactions, and approximation and alignment between the substrate and CeO_2 .

The DFT calculation demonstrated that 2-cyanopyridine is adsorbed on CeO_2 via multiple interactions, and preferable approximation and alignment of nitrile group of the substrate to OH group on CeO_2 are also brought about at the same time.

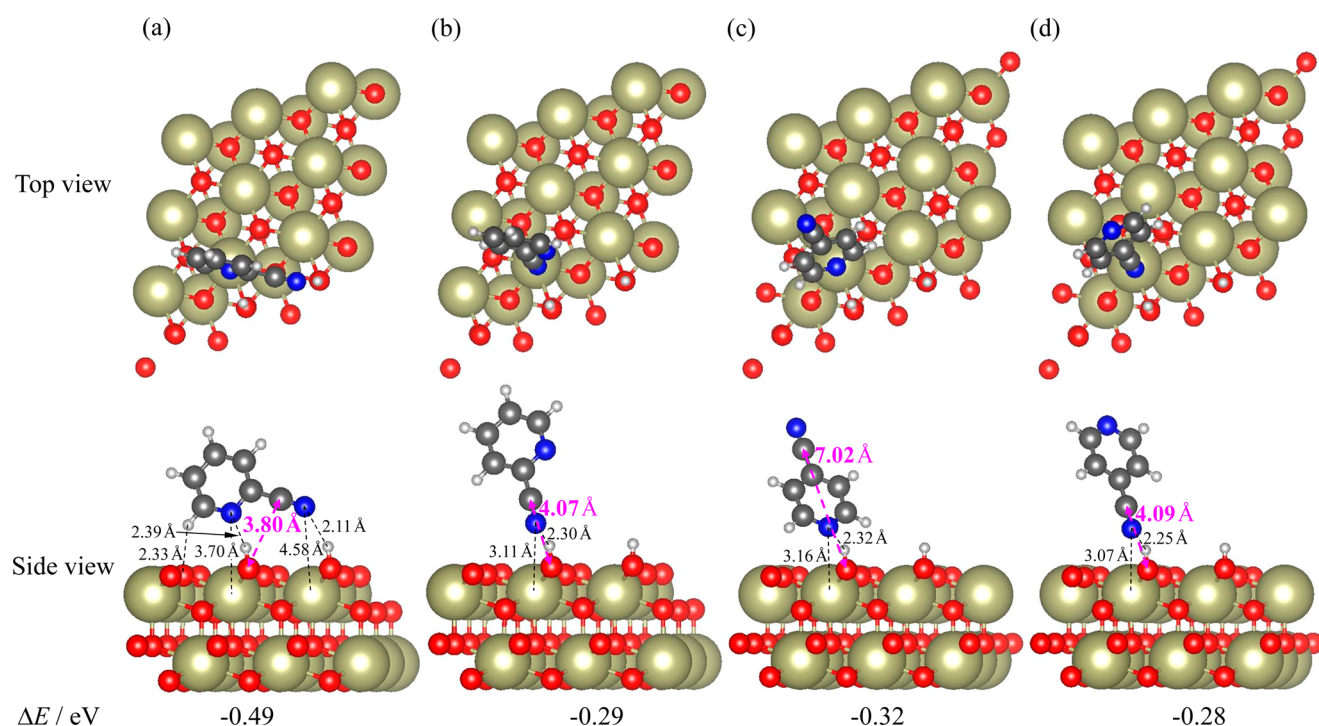


Figure 2. Optimized structures of 2-cyanopyridine and 4-cyanopyridine adsorption on CeO₂(111): (a) N_{pyridine} and (b) N_{nitrile} of 2-cyanopyridine, and (c) N_{pyridine} and (d) N_{nitrile} of 4-cyanopyridine. Ce atoms are in yellow, O in red, C in gray, H in white, and N in blue.

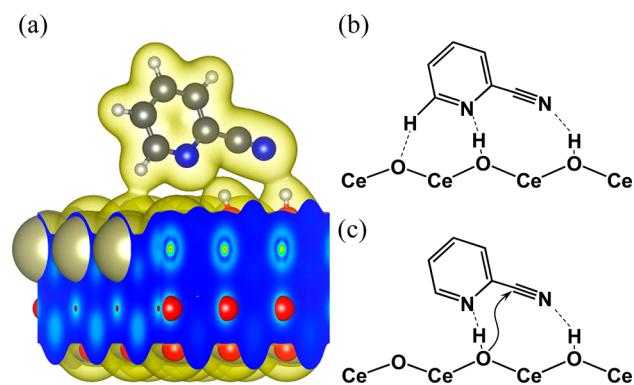


Figure 3. (a) Electron density contour (0.01 au⁻³) of the adsorption mode of 2-cyanopyridine. (b) Optimized adsorption image of 2-cyanopyridine on CeO₂. (c) Image of the rate-determining step.

Combination of these three factors will lead to the drastic rate enhancement for 2-cyanopyridine. Taking these results and reactivities of the substrates into consideration, we can conclude that the high substrate specificity is achieved by the multiple interactions, and approximation and alignment of the substrate with CeO₂.

3. CONCLUSIONS

We disclosed the origin of substrate specificity by clarifying the difference of reactivities between the reactive substrate and unreactive one in hydration of nitriles over CeO₂. From the results of the substrate scope, we confirmed that the reactive nitriles have a heteroatom (N or O) adjacent to the CN group and no steric hindrance around a heteroatom (N or O). The reaction rate of 2-cyanopyridine is 10⁷ times higher than that of 4-cyanopyridine, which is comparable to the difference of reactivities between the catalyzed substrate and noncatalyzed one in biological systems. Kinetic studies and DFT calculations

by comparing the reactive substrate, 2-cyanopyridine, with the unreactive substrate, 4-cyanopyridine, demonstrated that the difference in reactivity is derived from the large activation entropy gap between these substrates. The dramatic reduction of the activation entropy is induced by multiple interactions between the reactive substrate and CeO₂ surface, and approximation and alignment of the nitrile group of the substrates to OH group on CeO₂ surface. These phenomena resulted in enhancement of the reactivity of the reactive nitriles, which arises large difference of reactivities between the reactive and unreactive nitriles. This mechanism of substrate specificity will provide the clues for clarifying the catalyst mechanism in biological systems. In addition, the fact that nonporous metal oxides can precisely recognize the substrate by multiple interactions will provide a new possibility of heterogeneous catalysts in design of new catalysts and open up a wide range of new potential applications of CeO₂ in organic synthesis and chemistry of catalysis.

4. EXPERIMENTAL SECTION

General. The samples were analyzed by GC (Shimadzu GC-14B) and GCMS (Shimadzu GCMS-QP5000) with Ultra-alloy metal capillary column (Frontier Laboratories Ltd.) under nitrogen carrier gas. All the chemicals used for organic reactions were of analytical grades and purchased from chemical corporations. They were used without further purification.

Catalyst. CeO₂ (JRC-CEO-3), which was precalcined at 600 °C before being supplied, was supplied from Catalysis Society of Japan. The surface area of CeO₂ was 81 m²/g. The purity of CeO₂ (JRC-CEO-3) is 99.97%.

Typical Procedure for Hydration of Nitriles over CeO₂. Hydration of 2-cyanopyridine to 2-picolinamide over CeO₂ was performed as follows. 2-Cyanopyridine (0.2g, 2.0 mmol) and H₂O (3.0g, 0.17 mol) were added to a reaction vessel equipped with a condenser, and then 30 mg of CeO₂ (0.17 mmol, 8.7 mol

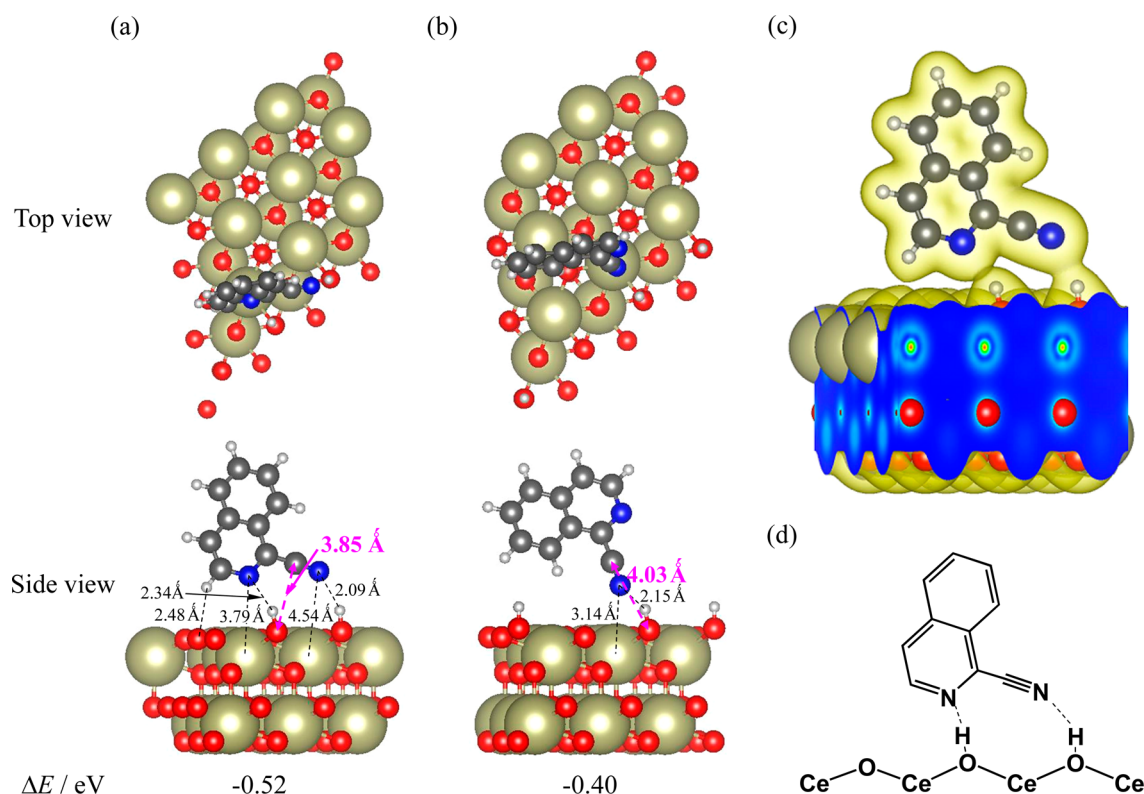


Figure 4. Optimized structures of 1-isoquinolinecarbonitrile adsorption on CeO₂(111) at (a) N_{pyridine} and (b) N_{nitrile} of 1-isoquinolinecarbonitrile: Ce atoms are in yellow, O in red, C in gray, H in white and N in blue. (c) Electron density contour (0.01 au⁻³) of the adsorption mode of 1-isoquinolinecarbonitrile. (d) Optimized adsorption image of 1-isoquinolinecarbonitrile on CeO₂.

% Ce with respect to 2-cyanopyridine) was added to the mixture. The obtained suspension was vigorously stirred under air at 30 °C in the desired reaction time. After the reaction, benzonitrile, an internal standard, was added to the reaction mixture, and immediately the reaction mixture was extracted thrice with 3 mL of CHCl₃; the obtained CHCl₃ layer was then analyzed by GC. When cyanopyrazine was used as a substrate, methanol (6 mL) was added into the resulting reaction mixture in order to dissolve pyrazinecarboxamide, which is a hydration product of cyanopyrazine. Conversion and yield in hydration of 2-cyanopyridine were determined on the basis of 2-cyanopyridine and picolinamide by GC with the internal standard of benzonitrile. In the case of cyanopyrazine, 1-hexanol was used as an internal standard. The produced amides were identified by GCMS on the basis of the molecular ion peak and fragmentation peaks. Additionally, they were also compared with commercially pure products.

Calculation. Adsorbed Structure. Calculations for nitrile adsorption on CeO₂ surfaces were performed within the framework of spin-polarized density functional theory (DFT), as implemented in the PWscf code of the Quantum ESPRESSO package.²² For this calculation, the generalized gradient approximation in the formulation of Perdew–Burke–Ernzerhof²³ was used to represent the exchange correlation functional. A basis set of plane waves was limited by an energy cutoff of 30 Ry, while the cutoff for the electron density representation was set to 300 Ry. The Hubbard U parameter²⁴ of 1.5 eV was employed for the inclusion of on-site Coulomb interaction of Ce atoms. The ultrasoft type of Vanderbilt pseudopotential²⁵ was used for the treatment of core electrons. Integrals in the Brillouin zone were performed on Monkhorst–Pack mesh of (2 × 2 × 1) k-points²⁶ together with the Methfessel–Paxton smearing width²⁷ of 0.01 Ry. The CeO₂(111) surface was represented by the slab

model of (3 × 3) lateral cells with six atomic layers. Each slab was separated by a vacuum space of 16 Å. During the geometry optimization, the lowermost three layers were kept fixed at the bulk coordinates. Relative energies (ΔE) were defined as the energy of the adsorbed system relative to that of the sum of the isolated system. All pictures of optimized structures and electron densities are drawn by VESTA.²⁸

■ ASSOCIATED CONTENT

Supporting Information

The following file is available free of charge on the ACS Publications website at DOI: 10.1021/cs501448n.

Results of Arrhenius plots and optimization of adsorption sites by DFT calculations (PDF)

■ AUTHOR INFORMATION

Corresponding Authors

*E-mail: mtamura@erec.che.tohoku.ac.jp.

*E-mail: kshimizu@cat.hokudai.ac.jp.

Notes

The authors declare no competing financial interest.

■ ACKNOWLEDGMENTS

The present work was (partially) supported by MEXT program “Elements Strategy Initiative to Form Core Research Center”, MEXT; Ministry of Education Culture, Sports, Science and Technology, Japan.

■ REFERENCES

- (1) Kirby, A. J.; Hollfelder, F. *From Enzyme Models to Model Enzymes*; RSC Publishing, Cambridge, U.K., 2009.
- (2) Nanda, V.;

Koder, R. L. *Nat. Chem.* **2009**, *2*, 15–24. (c) Breslow, R., Ed. *Artificial Enzymes*; Wiley-VCH: Weinheim, 2005.

(2) (a) Das, S.; Brudvig, G. W.; Crabtree, R. H. *Chem. Commun.* **2008**, 413–424. (b) Suh, J. *Acc. Chem. Res.* **2003**, *36*, 562–570. (c) Lee, T. Y.; Suh, J. *Chem. Soc. Rev.* **2009**, *38*, 1949–1957. (d) Fenger, T. H.; Bols, M. *Chem. Commun.* **2010**, *46*, 7769–7771. (e) Marinescu, L. G.; Bols, M. *Angew. Chem., Int. Ed.* **2006**, *45*, 4590–4593. (f) Maruoka, K.; Saito, S.; Concepcion, A. B.; Yamamoto, H. *J. Am. Chem. Soc.* **1993**, *115*, 1183–1184. (g) Nakajima, H.; Yasuda, M.; Takeda, R.; Baba, A. *Angew. Chem., Int. Ed.* **2012**, *51*, 3867–3870. (h) Kunishima, M.; Yoshimura, K.; Morigaki, H.; Kawamata, R.; Terao, K.; Tani, S. *J. Am. Chem. Soc.* **2001**, *123*, 10760–10761. (i) Wulff, G. *Chem. Rev.* **2002**, *102*, 1–27. (j) Wulff, G.; Liu, J. *Acc. Chem. Res.* **2012**, *45*, 239–247. (k) Nanda, V.; Koder, R. L. *Nat. Chem.* **2010**, *2*, 15–24. (l) Becker, J. J.; Gagne, M. R. *Acc. Chem. Res.* **2004**, *37*, 798–804. (m) Yoshizawa, M.; Tamura, M.; Fujita, M. *Science* **2006**, *312*, 251–254. (n) Smejkal, T.; Breit, B. *Angew. Chem., Int. Ed.* **2008**, *47*, 311–315. (o) Sun, X.; Lee, H.; Tan, K. L. *Nat. Chem.* **2013**, *5*, 790–795. (p) Ooe, M.; Murata, M.; Mizugaki, T.; Ebitani, K.; Kaneda, K. *Nano Lett.* **2002**, *2*, 999–1002.

(3) (a) Haag, W. O.; Lago, R. M.; Weisz, P. B. *Faraday Disc. Chem. Soc.* **1982**, *72*, 317–330. (b) Niwa, M.; Kato, M.; Hattori, T.; Murakami, Y. *J. Phys. Chem.* **1986**, *90*, 6233–6237.

(4) Yoshinaga, Y.; Seki, K.; Nakato, T.; Okuhara, T. *Angew. Chem., Int. Ed.* **1997**, *36*, 2833–2835.

(5) Inumaru, K.; Kasahara, T.; Yasui, M.; Yamanaka, S. *Chem. Commun.* **2005**, 2131–2133.

(6) Shiraiishi, Y.; Tsukamoto, D.; Hirai, T. *Langmuir* **2008**, *24*, 12658–12663.

(7) (a) Jones, C. W.; Tsuji, K.; Davis, M. E. *Nature* **1998**, *393*, 52–54. (b) Zapilko, C.; Liang, Y.; Nerdal, W.; Anwander, R. *Chem.—Eur. J.* **2007**, *13*, 3169–3176.

(8) (a) Tada, M.; Iwasawa, Y. *Chem. Commun.* **2006**, 2833–2844. (b) Tada, M.; Sasaki, T.; Iwasawa, Y. *Phys. Chem. Chem. Phys.* **2002**, *4*, 4561–4574. (c) Yang, Y.; Weng, Z.; Muratsugu, S.; Ishiguro, N.; Ohkoshi, S.-i.; Tada, M. *Chem.—Eur. J.* **2012**, *18*, 1142–1153.

(9) Katz, A.; Davis, M. E. *Nature* **2000**, *403*, 286–289.

(10) (a) Lightstone, F. C.; Bruice, T. C. *J. Am. Chem. Soc.* **1996**, *118*, 2595–2605. (b) Herschlag, D.; Natarajan, A. *Biochemistry* **2013**, *52*, 2050–2067. (c) Houck, W. J.; Pollack, R. M. *J. Am. Chem. Soc.* **2003**, *125*, 10206–10212. (d) Trobro, S.; Åqvist, J. *Proc. Natl. Acad. Sci. U.S.A.* **2005**, *102*, 12395–12400. (e) Villà, J.; Štrajbl, J. V.; Glennon, T. M.; Sham, Y. Y.; Chu, Z. T.; Warshel, A. *Proc. Natl. Acad. Sci. U.S.A.* **2000**, *97*, 11899–11904.

(11) Schroeder, G. K.; Wolfenden, R. *Biochemistry* **2007**, *46*, 4037–4044.

(12) Sievers, A.; Beringer, M.; Rodnina, M. V.; Wolfenden, R. *Proc. Natl. Acad. Sci. U.S.A.* **2004**, *101*, 7897–7901.

(13) (a) Tamura, M.; Wakasugi, H.; Shimizu, K.-i.; Satsuma, A. *Chem.—Eur. J.* **2011**, *17*, 11428–11431. (b) Tamura, M.; Satsuma, A.; Shimizu, K.-i. *Catal. Sci. Technol.* **2013**, *3*, 1386–1393.

(14) Mitsudome, T.; Mikami, Y.; Mori, H.; Arita, S.; Mizugaki, T.; Jitsukawa, K.; Kaneda, K. *Chem. Commun.* **2009**, 3258–3260.

(15) (a) Storm, D. R.; Koshland, D. E., Jr. *Proc. Natl. Acad. Sci. U.S.A.* **1970**, *66*, 445–452. (b) Storm, D. R.; Koshland, D. E., Jr. *J. Am. Chem. Soc.* **1972**, *94*, 5815–5825. (c) Wallin, G.; Åqvist, J. *Proc. Natl. Acad. Sci. U.S.A.* **2010**, *107*, 1888–1893.

(16) (a) Hur, S.; Bruice, T. C. *J. Am. Chem. Soc.* **2003**, *125*, 10540–10542. (b) Hur, S.; Bruice, T. C. *Proc. Natl. Acad. Sci. U.S.A.* **2003**, *100*, 12015–12020.

(17) (a) Ichikawa, N.; Sato, S.; Takahashi, R.; Sodesawa, T.; Fujita, H.; Atoguchi, T.; Shiga, A. *J. Catal.* **2006**, *239*, 13–22. (b) Sawabe, K.; Yoshikawa, Y.; Satsuma, A. *Top. Catal.* **2014**, *57*, 1094–1102. (c) Li, M.; Wu, Zili; Overbury, S. H. *J. Catal.* **2013**, *306*, 164–176.

(18) Tamura, M.; Shimizu, K.-i.; Satsuma, A. *Appl. Catal., A* **2012**, *433–434*, 135–145.

(19) Geometry optimization was also carried out using the initial structure at which 2-cyanopyridine was located with its pyridine ring parallel to the ideal CeO₂ surface. After several optimization cycles, the

pyridine ring of 2-cyanopyridine got up from the surface. Therefore, there is no adsorption configuration with its ring parallel to the surface.

(20) Alkorta, I. R.; Elguero, J. *Struct. Chem.* **1998**, *9*, 243–247.

(21) The adsorption through N pyridine is more preferable, multiple interactions between the substrate and CeO₂ are formed, and the distance and position between the reacting atoms (C of CN in 1-isoquinolinecarbonitrile and O of OH on CeO₂) is closer and favorable (Figure 4).

(22) Giannozzi, P.; Baroni, S.; Bonini, N.; Calandra, M.; Car, R.; Cavazzoni, C.; Ceresoli, D.; Chiarotti, G. L.; Cococcioni, M.; Dabo, I.; Corso, A. D.; Gironcoli, S. D.; Fabris, S.; Fratesi, G.; Gebauer, R.; Gerstmann, U.; Gougoussis, C.; Kokalj, A.; Lazzeri, M.; Martin-samos, L.; Marzari, N.; Mauri, F.; Mazzarello, R.; Paolini, S.; Pasquarello, A.; Paulatto, L.; Sbraccia, C.; Scandolo, S.; Sclauzero, G.; Seitsonen, A. P.; Smogunov, A.; Umari, P.; Wentzcovitch, R. M. *J. Phys.: Condens. Matter* **2009**, *21*, 395502–1–395502–19.

(23) Perdew, J. P.; Burke, K.; Ernzerhof, M. *Phys. Rev. Lett.* **1996**, *77*, 3865–3868.

(24) Cococcioni, M.; Gironcoli, S. D. *Phys. Rev. B* **2005**, *71*, 035105–1–035105–16.

(25) Vanderbilt, D. *Phys. Rev. B* **1990**, *41*, R7892–R7895.

(26) Monkhorst, H. J.; Pack, J. D. *Phys. Rev. B* **1976**, *13*, 5188–5192.

(27) Methfessel, M.; Paxton, A. T. *Phys. Rev. B* **1989**, *40*, 3616–3621.

(28) Momma, K.; Izumi, F. *J. Appl. Crystallogr.* **2011**, *44*, 1272–1276.